Biochemical and Biophysical Research Communications 421 (2012) 449–455

Contents lists available at SciVerse ScienceDirect

Biochemical and Biophysical Research Communications

journal homepage: www.elsevier.com/locate/ybbrc

Iron repletion relocalizes hephaestin to a proximal basolateral compartment in polarized MDCK and Caco2 cells

Seung-Min Lee [a,f], Zouhair K. Attieh [b,f], Hee Sook Son [c,f], Huijun Chen [d,f], Mhenia Bacouri-Haidar [e,f] Chris D. Vulpe [f,*]

[a] Department of Biological Sciences, University of Columbia, NY, USA
[b] Department of Laboratory Science and Technology, American University of Science and Technology, Ashrafieh, Lebanon
[c] Department of Food Science and Human Nutrition, College of Human Ecology, Chonbuk National University, South Korea
[d] Medical School, Nanjing University, Nanjing 210008, Jiangsu Province, China
[e] Department of Biology, Faculty of Sciences (I), Lebanese University, Hadath, Lebanon
[f] Department of Nutritional Science and Toxicology, University of California, Berkeley, CA, USA

ARTICLE INFO

Article history:
Received 23 March 2012
Available online 7 April 2012

Keywords:
Copper
Iron
Hephaestin
Ferroportin
Apo-transferrin
Holo-transferrin
Enterocytes

ABSTRACT

While intestinal cellular iron entry in vertebrates employs multiple routes including heme and non-heme routes, iron egress from these cells is exclusively channeled through the only known transporter, ferroportin. Reduced intestinal iron export in sex-linked anemia mice implicates hephaestin, a ferroxidase, in this process. Polarized cells are exposed to two distinct environments. Enterocytes contact the gut lumen via the apical surface of the cell, and through the basolateral surface, to the body. Previous studies indicate both local and systemic control of iron uptake. We hypothesized that differences in iron availability at the apical and/or basolateral surface may modulate iron uptake via cellular localization of hephaestin. We therefore characterized the localization of hephaestin in two models of polarized epithelial cell lines, MDCK and Caco2, with varying iron availability at the apical and basolateral surfaces. Our results indicate that hephaestin is expressed in a supra-nuclear compartment in non-polarized cells regardless of the iron status of the cells and in iron deficient and polarized cells. In polarized cells, we found that both apical (as $FeSO_4$) and basolateral iron (as the ratio of apo-transferrin to holo-transferrin) affect mobilization of hephaestin from the supra-nuclear compartment. We find that the presence of apical iron is essential for relocalization of hephaestin to a cellular compartment in close proximity but not overlapping with the basolateral surface. Surface biotinylation studies indicate that hephaestin in the peri-basolateral location is accessible to the extra-cellular environment. These results support the hypothesis that hephaestin is involved in iron mobilization of iron from the intestine to circulation.

1. Introduction

Iron, essential for many biological reactions, is toxic when in excess. Cells have developed elaborate mechanisms for iron uptake, mobilization and storage, as the ability of the body to excrete iron is limited [1]. Iron enters the body through the intestinal epithelium through the divalent metal transporter 1 (DMT1) [2] facilitated by a proposed ferric reductase [3]. Once inside cells, Fe is trancytosed to the basolateral side where the iron transporter ferroportin (FPN) directs its movement out of the cells eventually into circulation to be bound to transferrin (Tf) [4]. The membrane bound ferroxidase hephaestin (Heph), originally identified from study of sex-linked anemia (*sla*) mice, is believed to facilitate iron egress by oxidizing the soluble ferrous iron into the ferric state prior to its release by FPN [5].

The ferroxidase-permease mechanism for iron mobilization was first proposed in yeast where the yeast ferroxidase Fet3 oxidizes Fe^{2+} that is subsequently internalized into cells by Ftr [6]. In mammals, the ferroxidase ceruloplasmin has been shown to mediate iron efflux from various tissues and cells [7]. While the soluble form of ceruloplasmin (Cp) does not interact directly with a permease, the glycosylphosphatidylinisotol (GPI)-anchored form of the protein was shown to interact with FPN and the absence of GPI-Cp leads, analogous to the yeast model, to the failure of FPN to localize to the basolateral membrane and the subsequent targeting for

Abbreviations: apo-Tf, apotransferrin; holo-Tf, holotransferrin; Heph, hephaestin; Cp, ceruloplasmin; DMT1, divalent metal transporter 1; FPN, ferroportin.

* Corresponding author. Address: Department of Nutritional Science and Toxicology, University of California, 119 Morgan Hall, Berkeley, CA 94720, USA. Fax: +1 510 642 0535.
E-mail address: vulpe@berkeley.edu (C.D. Vulpe).

0006-291X/$ - see front matter © 2012 Elsevier Inc. All rights reserved.
http://dx.doi.org/10.1016/j.bbrc.2012.04.008

degradation [8]. In the intestine, a similar scenario is proposed in which hephaestin and ferroportin interact to mediate iron mobilization. Evidence for the role of Heph in iron trafficking from the intestinal epithelium is derived from studies in the sex-linked anemia and Fe and Cu regulation studies. *Sla* mice accumulate iron and partially active *sla* Heph fails to localize to the basolateral membrane, probably explaining the lack of iron release form these cells [9]. *Sla* and iron-deficient mouse enterocytes have elevated Heph and FPN protein levels [10]. Copper deficiency leads to a marked decrease in Heph expression and ferroxidase activity but results in increased FPN protein levels. Copper deficiency was also shown to result in lower Heph protein levels and Fe transport in Caco2 monolayers whereas no change in FPN protein expression was observed [11].

Heph is normally expressed in a supranuclear compartment in addition to the basolateral membrane [9]. Heph translocated to the basolateral membrane when rats were fed Fe-replete diet [12]. In addition, the basolateral targeting of Heph results in the interaction with FPN [12] which is reduced upon iron feeding [13]. Collectively, the data indicate that Heph translocation to the basolateral membrane is essential for its proper functioning in coordination with FPN effecting iron egress from the intestine to circulation.

In the current study, we have investigated the expression of Heph and localization in MDCK and Caco2 cell monolayers and found that Heph expression is confined to the supranuclear compartment in non-polarized cells regardless of available iron. In contrast, Heph translocates to a proximal basolateral compartment in polarized cultured MDCK and Caco2 cells in conditions of adequate apical iron and basolateral iron deficiency. Interestingly, Heph expression does not co-localize with the basolateral marker Na^+/K^+ ATPase but is still accessible to the extracellular milieu. Together these studies show a dynamic regulation of Heph localization by the local iron environment.

2. Materials and methods

2.1. Cell culture

MDCK cells were a kind gift from Dr. Jane Gitschier (University of California, San Francisco). Cells were grown minimum essential medium (MEM) with Earle's salts supplemented with 2 mM L-glutamine, 0.1 mM nonessential amino acids (NEAA), 1 mM sodium pyruvate, and 10% heat-inactivated fetal bovine serum (FBS). Prior to the experiments, 5×10^4 cells were seeded on 0.4 mm microporous polycarbonate membrane inserts (1 cm^2 Transwell inserts; Corning, Acton, MA). The medium on both sides of the filter insert in transwell plates was changed every 2 days. Transepithelial electrical resistance (TEER) was monitored to assess the formation of a tight cell monolayer, and the formation of a fully differentiated cell monolayer was typically established by days 6–7 with TEER > 250 V/cm^2. For transient overexpression studies, MDCK cells were transfected with a pcDNA3.1 plasmid encoding full-length Heph with the human cytomegalovirus immediate-early (CMV) promoter (a kind gift from Dr. Greg Anderson, University of Queensland, Brisbane, Queensland, Australia) with a FLAG epitope tag at the C terminus.

Caco2 cells were a kind gift from Dr. Paul Sharp (King's College, London) at passage 28 and used for experiments at passages 30–35. Caco2 cells were maintained in MEM with Earle's salts and L-glutamine supplemented with 10% FBS, 1% NEAA, 100 U/L penicillin G, and 100 mg/L streptomycin at 37 °C in a humidified atmosphere of 95% air and 5% CO_2. The growth medium was changed every second day. Culture in transwell plates and monolayer formation was performed as in MDCK cells above with the formation of a fully differentiated cell monolayer typically established by days 18–21 with TEER > 250 V/cm^2.

2.2. Cell treatment

Ferric ammonium citrate (FAC), desferrioxamine (DFO), bovine holo-transferrin (Holo-Tf) and bovine apo-Tf were purchased from Sigma–Aldrich (St. Louis, MO). For iron sufficient condition, 4 μM FAC was added into the cell culture medium. 100 μM of FAC and 100 μM of DFO were used to elicit iron overload and iron deficient conditions, respectively. Transwell plates allow separate access to the apical and basolateral surface of the cells. We individually adjusted the iron content of the media in each (the apical and basolateral) chamber to mimic different possible physiologic scenarios (e.g. iron deficient diet/systemic iron deficiency). To mimic systemic iron deficiency, bovine apo-Tf was added to a lower compartment of the transwell at the concentration of 3.8 μM. Conversely, 3.8 μM of bovine holo-Tf was added to the lower compartment of the transwell to mimic systemic iron sufficiency.

2.3. Cell lysis and immunoblot analysis

Cells were scraped into lysis buffer and were incubated on ice for 30 min. After being extruded through a 27-gauge needle 10 times, cell lysates were centrifuged at 10,000*g* for 20 min at 4 °C. Total protein in cell supernatants was quantified using the Bradford method (Bio-Rad, Richmond, CA). Protein extracts were resolved on 4–12% Tris–glycine polyacrylamide gels (PAGE) (Invitrogen, Carlsbad, CA) and then transferred to a polyvinylidene difluoride (PVDF) membrane. Heph was detected using polyclonal rabbit anti-mouse Ab (Hp2) (1:1000) with horseradish peroxidase-conjugated goat anti-rabbit IgG (1:15,000) (Santa Cruz Biotech, Santa Cruz, CA) and enhanced chemiluminescence (ECL, Amersham Biosciences Inc, Piscataway, NJ). Hp2 was raised against an oligopeptide, AFQDETFQERVHQEEETH (residues 334–451), derived from the extracellular domain of hephaestin [14].

2.4. Immunocytochemistry

Cell monolayers were washed with PBS and fixed in 4% formaldehyde solution for 30 min at room temperature (RT). Nonspecific binding sites were blocked by incubating cells in 10% FBS and 0.1% saponin in PBS. Cells were incubated with Hp2 antibody for 2 h, and then with Alexa488-conjugated goat anti-rabbit antibody (Santa Cruiz Biotechnology, Santa Cruz, CA) for 1 h. Nuclei were stained with DAPI for 15 min. Transwell membranes were washed, excised, and mounted on a glass slide. Cells were observed by confocal microcopy at the UCB bioimaging facility using Zeiss 510 UV/Vis Meta (Carl Zeiss Inc., Thornwood, NY).

2.5. Surface staining of Heph

Caco2 cell monolayers grown on transwell plates were washed with ice-cold PBS containing 1 mM $CaCl_2$ and 0.5 mM $MgCl_2$ and then biotinylated on either the apical or the basolateral surface with 1 mg/ml sulfosuccinimidyl 2-ethyl-1,3-dithiopropionate (EZ-Link® Sulfo-NHS-SS-biotin, Pierce, USA) in PBS (pH 9.0) at 4 °C for 1 h. After the biotinylation reaction was quenched with quenching solution (Pierce, USA), the cells were washed with ice-cold PBS and lysed on ice for 30 min and extruded through a 27 gauge needle 3–5 times. Cellular debris was removed by centrifugation at 8000*g* for 20 min at 4 °C. Biotinylated proteins were immunoprecipitated with an Immobilized Neutravidin™ gel slurry by incubating overnight at 4 °C. In order to elute proteins, the gel slurry was mixed with SDS–PAGE sample buffer containing 50 mM DTT and incubated for 1 h

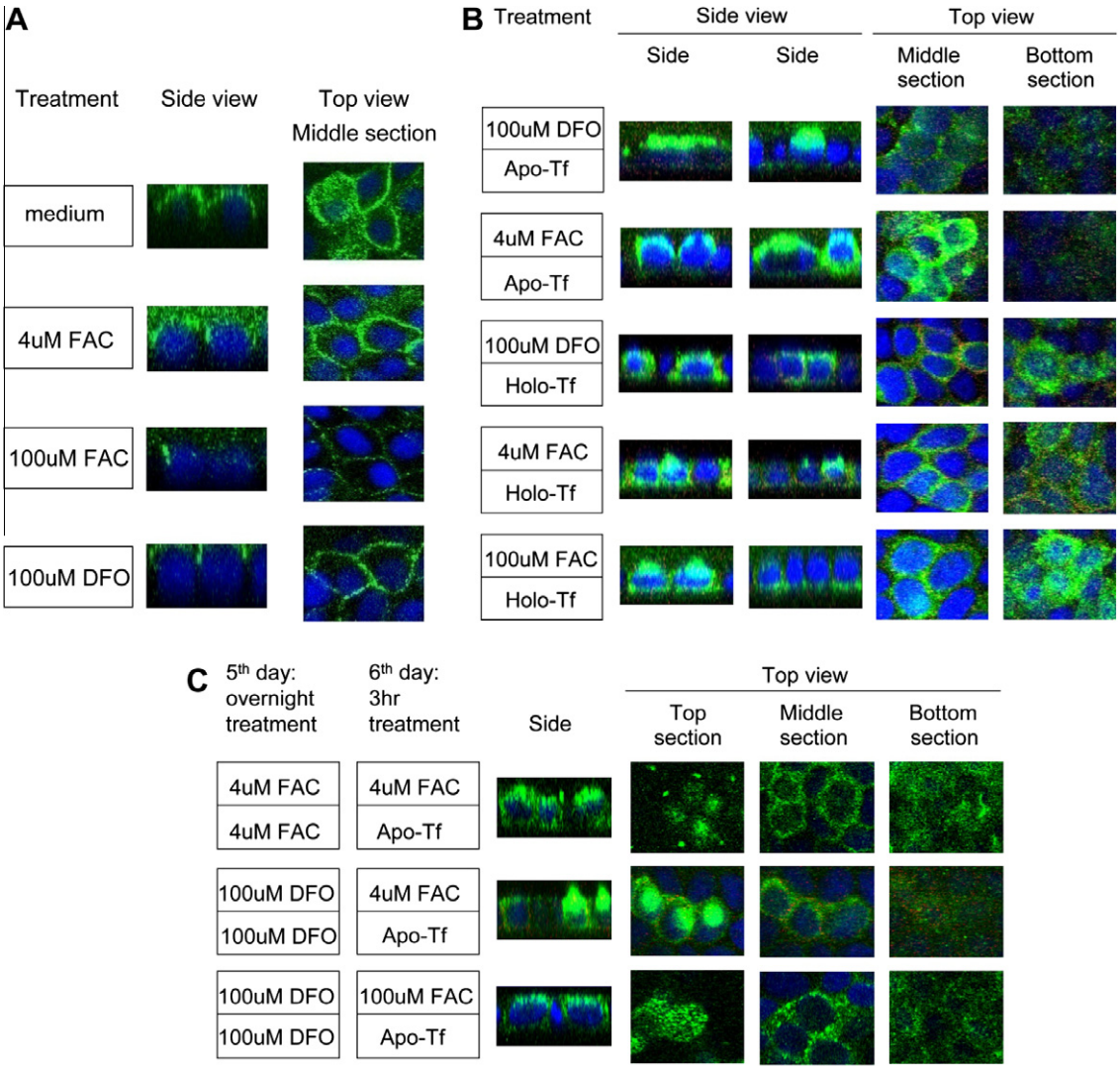

Fig. 1. Localization of Heph in MDCK cells. (A) Localization of Heph in non-polarized MDCK cells. MDCK cells were transfected with a construct expressing Heph. Left column indicates the conditions used in both the upper and lower compartments. Cells were immunostained for Heph (green). Nuclei are stained with DAPI (blue). (B) Localization of Heph in polarized MDCK cells. MDCK cells were grown on transwell membranes and transfected with Heph construct 4 days after seeding a confluent number of cells. At day 6, the medium in the upper chamber was replaced by fresh medium containing FAC or DFO. In the lower compartment, apo-Tf or holo-Tf was added to the fresh medium. Left column indicates the conditions used in the upper and lower compartments. Heph is shown in green and the nucleus is stained in blue. (C) Localization of Heph in iron deficient MDCK cells. Polarized MDCK cells were transfected with Heph construct at day 4 after seeding and then treated with the iron chelator, DFO overnight. At day 6, cells were treated with iron and apo-Tf according to the conditions indicated in the left columns. Cells were fixed after 3 h of treatment and stained for Heph (green) and nucleus (blue). (For interpretation of the references to color in this figure legend, the reader is referred to the web version of this article.)

at RT before centrifugation. The supernatant was collected and used for immunoblotting.

3. Results

3.1. Heph localization in non-polarized MDCK cells

We investigated the localization of Heph in non-polarized MDCK cells using anti-Heph antibody (Hp2). We noted that culture of MDCK for 24 h in medium containing 10% FBS (complete medium) results in marked increase in Tfr1 expression which is indicative of iron deficiency. In order to find conditions of cellular iron sufficiency, we titrated FAC and found that addition of 4 μM FAC to the medium was the minimal concentration to suppress Tfr1 expression. Therefore the MDCK cells were treated with 4 μM FAC to mimic iron sufficient conditions (IS), while 100 μM FAC and 100 μM DFO were used to mimic iron overload (IO) and iron deficient conditions (ID), respectively. Supranuclear staining was detected in cells either grown in complete medium or complete medium supplemented with 4 μM FAC, 100 μM FAC, 100 μM DFO (Fig. 1A) using Hp2 antibody. Regardless of the iron status of the non-polarized cells, Heph was not detected basolaterally.

3.2. Apical and basolateral iron affects Heph localization in polarized MDCK cells

We subsequently determined the localization of transiently expressed Heph in polarized MDCK cells grown in transwell plates. We added either apo-Tf or holo-Tf in the basolateral compartment to generate a different apo-Tf/holo-Tf ratio. Heph was detected in supra-nucleus compartment with 100 μM DFO in the apical compartment but was also detected laterally upon the addition of either 4 or 100 μM of FAC in the apical compartment (Fig. 1B). With holo-Tf in the basolateral compartment, Heph was detected on both the apical and basolateral side (Fig. 1B). Overall, primarily supranuclear staining with limited basolateral staining of Heph

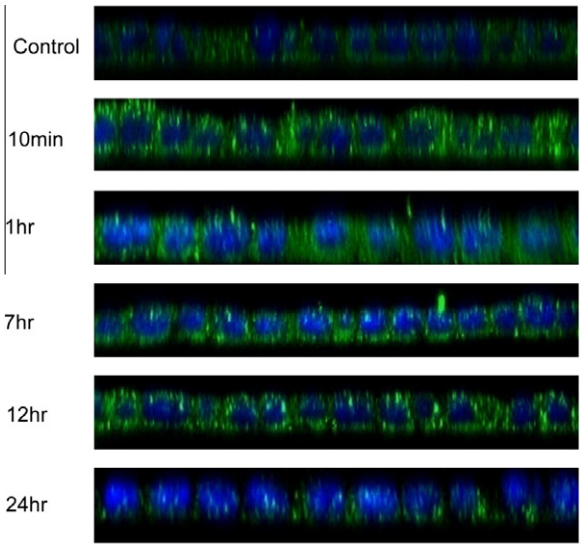

Fig. 2. Time course of changes in endogenous Heph localization in polarized MDCK cells. Polarized MDCK cells were treated with 50 μM FAC in the apical side and apo-Tf in the basal side and examined over 24 h. At indicated time points, cells were fixed and immunostained for Heph (green). Nuclei are stained with DAPI (blue). (For interpretation of the references to color in this figure legend, the reader is referred to the web version of this article.)

was detected in iron deficient cells upon treatment with 100 μM DFO on the apical side and addition of apo-Tf on the basolateral side (Fig. 1B).

3.3. Iron status of polarized MDCK cells modulates Heph localization

We investigated whether the iron status of polarized MDCK cells influences the localization of Heph. After transient transfection with Heph, cells were pre-treated with 4 μM FAC or 100 μM DFO overnight to make cells iron sufficient or iron deficient, respectively. We then added either 4 or 100 μM FAC to the apical compartment and 3.8 μM apo-Tf to the basal side. We observed supranuclear and basolateral staining of Heph in iron sufficient condition (Fig. 1C). However, we found a reduced Heph staining on the basal side of iron deficient cells as compared to iron sufficient cells regardless of subsequent iron treatment (Fig. 1C).

3.4. Endogenous Heph localization in polarized MDCK cells over time

We tested the localization of endogenous Heph in polarized and iron sufficient MDCK cells over a 24 h period. To induce relocalization of Heph, 50 μM FAC and 3.8 μM apo-Tf were added to the apical and basal compartments, respectively. After 10 min, Heph was detected all around the nuclei. One hour post-treatment, Heph was detected near the basolateral sides of the cells only without

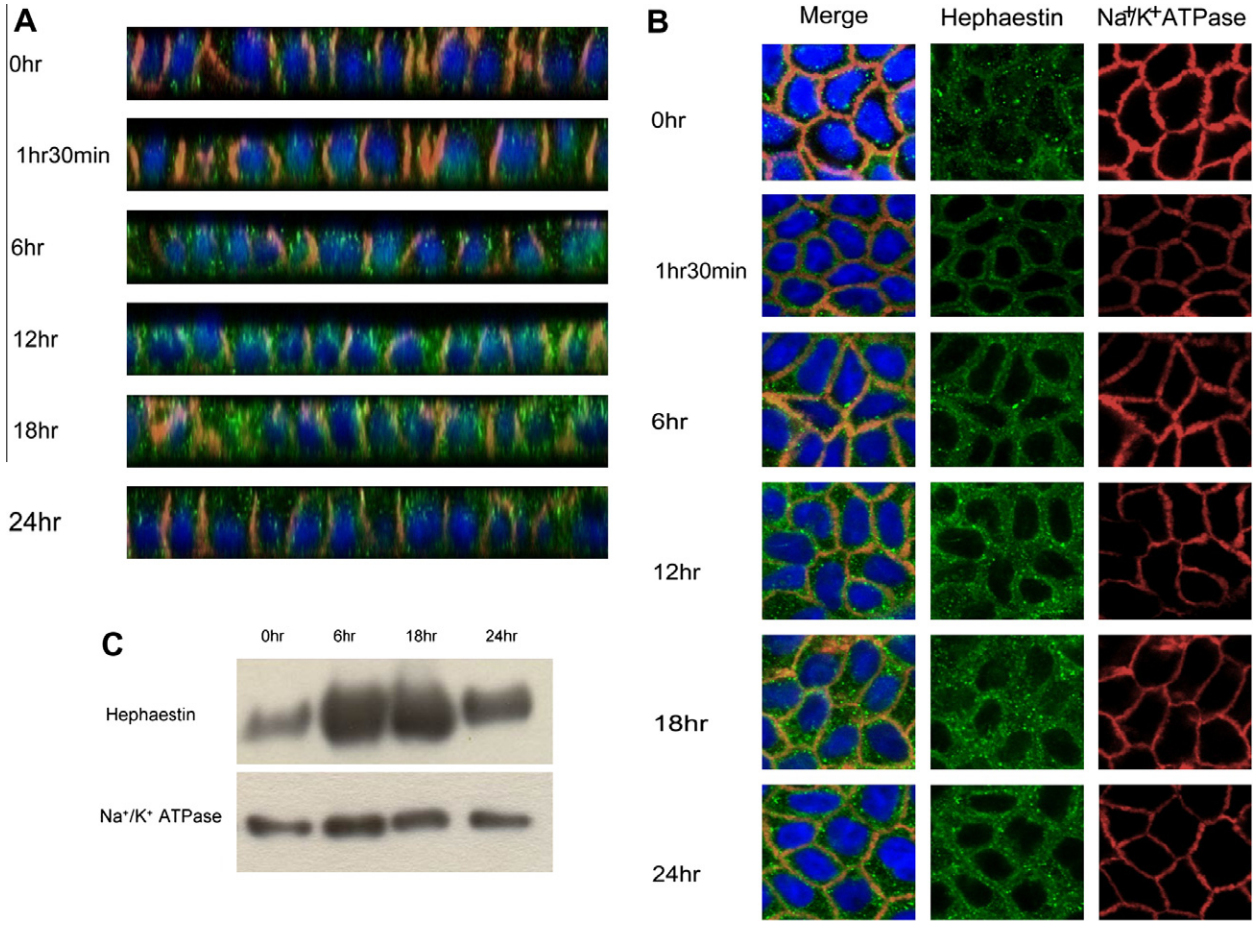

Fig. 3. Lack of complete co-localization of endogenous Heph with Na^+/K^+ ATPase in polarized cells. Side views (A) and middle section from the top view (B) of co-staining of endogenous Heph and Na^+/K^+ ATPase in polarized Caco2 cells. Caco2 cells were grown about 21 days on transwell membrane and then treated with 50 μM FAC in the upper compartment and with complete medium in the lower compartment. Staining of Heph (green) and Na^+/K^+ ATPase (red) was detected using confocal microscopy. The nuclei were visualized with DAPI staining (blue). (C) Detection of endogenous Heph from the basolateral side. Polarized Caco2 cells grown on transwell filter were biotinylated from the basolateral compartment. Surface proteins were immunoprecipitated with avidin before being subjected to Western blotting. Surface accessibility to Heph and Na^+/K^+ ATPase was examined by using the respective antibodies. (For interpretation of the references to color in this figure legend, the reader is referred to the web version of this article.)

A

```
R:EGNVKMLGMNIPVKNVEILSSALIAICVVLLLIALALGGVVWYQHRQRKLRRNNRRSILDDSFKLLSLKQ (1088-1157)
H:EGNVKMLGMQIPIKNVEMLASVLVAISVTLLLVVLALGGVVWYQHRQRKLRRNNRRSILDDSFKLLSFKQ (1089-1158)
M:GDNVKMLGMNIPIKDVEILSSALIAICVLLLLIALALGGVVWYQHRQRKLRRNNRRSILDDSFKLLSLKQ (1088-1157)
K:EGNVKMLGMQIPIKNVEILASVLVAIGVTLLLVVLALGGVVWYQHRQRKLRRNNRRSILDDSFKLLSFKQ (882-891)
C:EGSVKMLGMQIPIKDIEMLTSVLIAMGVILLLIALVLGGVVWYQHRQRKLRRNNRRSILDDSFKLLSLKQ (1089-1158)
D:EGNVRMLGMHIPIKNIDMLASVLISMSAILLLIALALGGVVWYQHRQRKLRRNNRRSILDDSFKLLSLKQ (1089-1158)
```

B

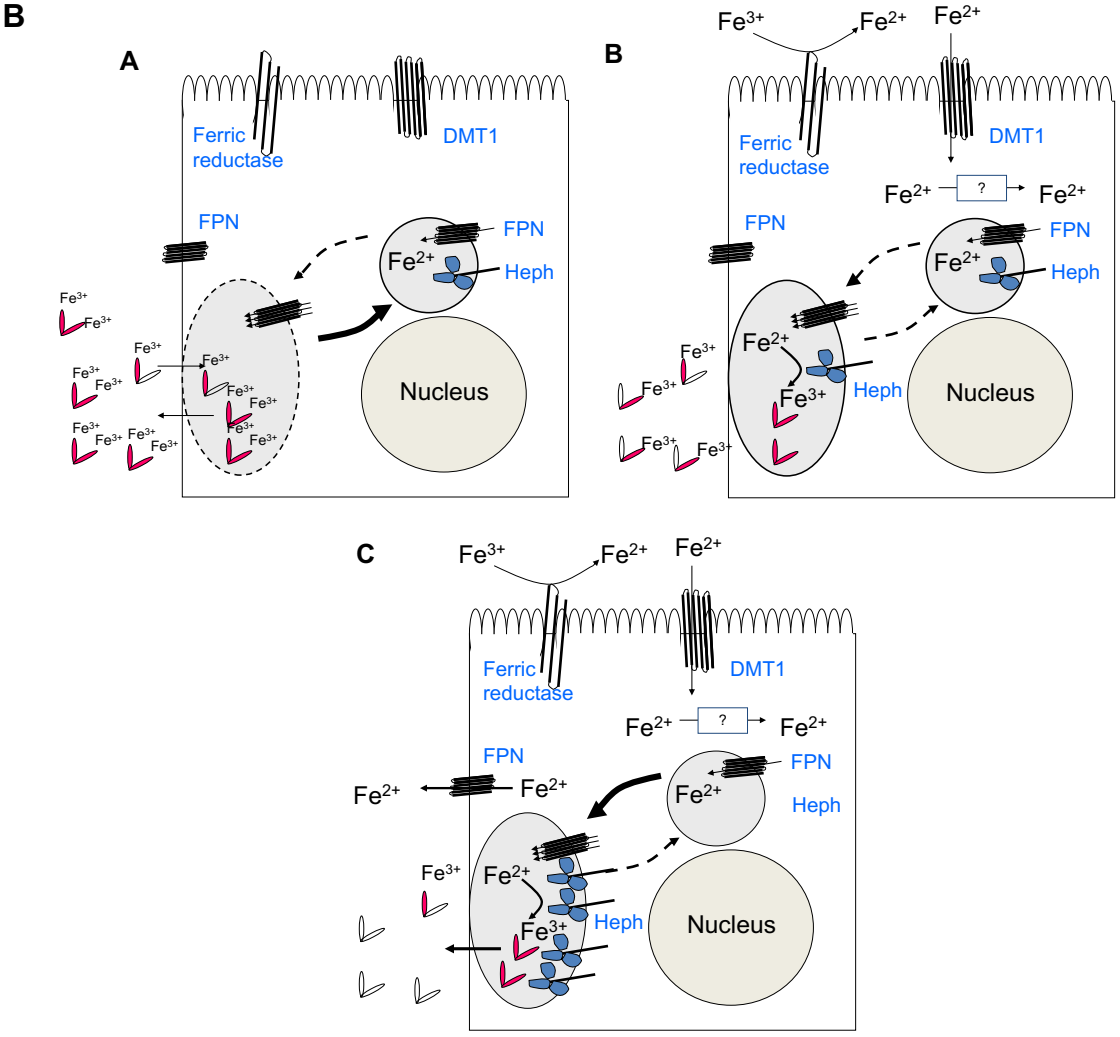

Fig. 4. Putative basolateral targeting signals in Heph and model of Heph in basolateral iron transport in enterocytes. (A) Conserved basolateral targeting motifs in Heph among species. Conserved amino acids are in red and basolateral motifs are in blue. R: rat (NP_579838), H: human (NP_620074), M: mouse (NP_034547), K: monkey (XP_001099362), C: cattle (XP_587920), D: dog (XP_549046). (B) Model of the role of Heph in transporting iron basolaterally in polarized cells. A – Iron transport without dietary iron on the apical side. B – Iron transport with dietary iron on the apical side and sufficient systemic iron (low ratio of apo-Tf to holo-Tf) on the basal side. C – Iron transport with high dietary iron and insufficient systemic iron (high ratio of apo-Tf to holo-Tf) on the basal side. Heph (hephaestin), FPN (ferroportin), and DMT1 (divalent metal transporter 1). ? symbol indicates an unknown mechanism.

supra-nuclear staining. This staining pattern was still apparent at 6 h after treatment while at 12 h, Heph was detected on all sides of the cells similar to the 10 min treatment. After 24 h of treatment, minimal staining of Heph was detected at the basal side (Fig. 2).

3.5. Heph does not completely co-localize with Na^+/K^+ ATPase

The changes in Heph localization in polarized MDCK cells were also observed in Caco2 cells (data not shown), a model for intestinal epithelial cells. Next, we performed a co-localization study of Heph utilizing the Na^+/K^+ ATPase as a basolateral membrane marker protein in polarized Caco2 cells. First, polarized Caco2 cells were treated with 50 μM FAC on the apical side. Treated cells were fixed at various time points over 24 h and co-stained using Heph (green) and Na^+/K^+ ATPase (red) antibodies. Characteristic lateral membrane staining of Na^+/K^+ ATPase was observed (Fig. 3A). At all time points, the lateral Heph staining does not appear to overlap with the Na^+/K^+ ATPase lateral staining in polarized Caco2 cells (Fig. 3A and B). Co-staining of Heph with Na^+/K^+ ATPase revealed that Heph staining does not completely overlap with Na^+/K^+ ATPase (Fig. 3A and B). The similar non-overlapping staining of Heph and Na^+/K^+ ATPase was observed as well (data not shown).

3.6. Heph accessible to surface biotinylation

The co-localization studies suggest that the majority of Heph is not present on the basolateral membrane but rather in a compartment in

close proximity. To determine if Heph is in contact with the extracellular milieu, we carried out a surface biotinylation study. Caco2 cell monolayers apically treated with 50 μM FAC were collected at 0, 6, 12, and 24 h post-treatment. Cell surface accessible proteins were biotinylated as described in methods. Biotinylated surface proteins were precipitated with Neutravidin and Heph was detected by immunoblotting with Heph IgG. As shown in Fig. 3C, the amount of Heph at the basolateral surface increased following 6 h of 50 μM FAC treatment on the apical side and lasted for at least 18 h. No significant change in the intensity of biotinylated Na^+/K^+ ATPase was observed over the course of the experiment. Thus the data indicate that the accessibility to Heph from basolateral compartment is modulated depending on apical iron availability.

4. Discussion

Previously, we showed that Heph is located primarily in an apical supranuclear compartment as well as on or near the basolateral membrane and demonstrated that Heph expression was increased in iron deficiency [14]. In this work we show that the localization of Heph changes in response to the availability of iron at the apical side of polarized cell lines. The changes in Heph localization were demonstrated by an increase in staining of Heph at the basolateral side of the cells both in MDCK and Caco2 cell lines. The addition of 3.8 μM apo-Tf in the basal compartment did not result in a significant increase in Heph basolateral staining compared to complete medium containing 10% FBS. Complete medium may contain 0.18∼0.22 mg/ml of Tf with varying degree of Tf saturation [15]. We found that Heph fails to localize to the basolateral sides of the cell in response to apical iron in the absence of steady state levels of intracellular iron. With sufficient amount of iron, Heph appears to be responsive to the availability of apical iron by changing its intracellular localization. In the presence of iron on the apical side, Heph relocalizes to the basolateral side of the iron sufficient cells. Interestingly, Heph does not colocalize with Na^+/K^+ ATPase, a basolateral membrane marker, suggesting that the majority of the protein is not present on the plasma membrane but rather in close proximity to the surface in an unknown compartment. Surface biotinylation data indicate that increasing amounts of Heph become accessible at the basolateral surface after addition of iron to the apical compartment. Our study suggests that Heph is present mainly in the perinuclear endomembrane compartment of the cell when there is no available iron for transcytosis. A combination of signals including the addition of iron at the apical side of the cell may trigger basolateral relocalization of Heph.

We examined the cytosolic part of the Heph sequence for putative basolateral targeting signals and identified two of them, one tyrosine type (YXXφ, φ: hydrophobic amino acids) and one dileucine-type (DDXXXLL) (Fig. 4A) [16]. Heph may regulate its cellular localization by utilizing one or more of these two putative basolateral targeting signals but direct evaluation of their role remains to be determined. These results and our previous studies in whole animals indicate that Heph is located both in a perinuclear compartment as well as on/or near the basolateral membrane in polarized cells. We propose a model of how Heph might be regulated in its localization to promote transcytosis of iron. As indicated in Fig. 4B, when dietary iron is absent, Heph is mainly localized in the upper compartment of the nucleus regardless of systemic iron status (Fig. 4B-A). However, when there is adequate dietary iron and sufficient systemic iron, Heph resides in both supranuclear compartment and basolateral side of the enterocytes (Fig. 4B-B). In systemic iron deficiency (low transferrin saturation) and sufficient dietary iron, hephaestin is primarily basolaterally (Fig. 4B-C).

We previously demonstrated that the *sla* mouse has decreased levels of a partially functional protein which is not detectable on/or near the basolateral surface. We observed no effect on FPN localization in *sla* mice. As the *sla* has a defect in iron egress from the intestinal cells, the decreased activity and/or lack of basolateral localization could explain the iron transport defect [9]. In this study, we showed that Heph relocalizes near the basolateral membrane and becomes surface accessible. Together these results suggest that basolateral localization of Heph may be important for a role of Heph in facilitating iron export. Heph has been shown to be a ferroxidase and we hypothesize that the ferroxidase activity is essential for the export process in conjunction with FPN. Previously, an interaction between FPN1 and Heph was shown in Caco2 cells [17]. Yeh et al. demonstrated that Heph and FPN interact directly in rat duodenal enterocytes [12] and recently the same group showed decreased interaction after iron feeding [13]. It would be interesting to consider the localization of Heph *in vivo* in response to iron feeding in iron deficient animals. The ferroxidase activity of Heph may maintain a local gradient of ferrous to ferric iron, which enables directional ferrous iron transport by FPN. A regulated localization process for hephaestin in response to apical iron could provide the means to regulate iron export only when dietary iron is available and prevent depletion of cellular stores.

Acknowledgments

The authors would like to acknowledge the technical help of Emily Su. This work was supported by NIH 5-R01-DK57800 and NIH 5-R01-DK56376 grants to CDV and Lebanese University Research and Development grant to MB-H.

References

[1] E.M. Widdowson, R.A. McCance, The absorption and excretion of iron before, during and after a period of very high intake, Biochem. J. 31 (1937) 2029–2034.
[2] H. Gunshin, M.A. Hediger (Eds.), The divalent metal-ion transporter (DCT1/DMT/Nramp2), Marcel Dekker, Inc., New York, 2002.
[3] A.T. McKie, D. Barrow, G.O. Latunde-Dada, A. Rolfs, G. Sager, E. Mudaly, M. Mudaly, C. Richardson, D. Barlow, A. Bomford, T.J. Peters, K.B. Raja, S. Shirali, M.A. Hediger, F. Farzaneh, R.J. Simpson, An iron-regulated ferric reductase associated with the absorption of dietary iron, Science 291 (2001) 1755–1759.
[4] A. Donovan, A. Brownlie, Y. Zhou, J. Shepard, S.J. Pratt, J. Moynihan, B.H. Paw, A. Drejer, B. Barut, A. Zapata, T.C. Law, C. Brugnara, S.E. Lux, G.S. Pinkus, J.L. Pinkus, P.D. Kingsley, J. Palis, M.D. Fleming, N.C. Andrews, L.I. Zon, Positional cloning of zebrafish ferroportin1 identifies a conserved vertebrate iron exporter, Nature 403 (2000) 776–781.
[5] C.D. Vulpe, Y.-M. Kuo, T.L. Murphy, L. Cowley, C. Askwith, N. Libina, J. Gitschier, G.J. Anderson, Hephaestin, a ceruloplasmin homologue implicated in intestinal iron transport, is defective in the sla mouse, Nat Genet. 21 (1999) 195–199.
[6] C. Askwith, D. Eide, A. Van Ho, P.S. Bernard, L. Li, S. Davis-Kaplan, D.M. Sipe, J. Kaplan, The FET3 gene of *S. cerevisiae* encodes a multicopper oxidase required for ferrous iron uptake, Cell. 76 (1994) 403–410.
[7] D.J. Kosman, Redox cycling in iron uptake, efflux, and trafficking, J. Biol. Chem. 285 (2010) 26729–26735.
[8] I. De Domenico, D.M. Ward, C. Langelier, M.B. Vaughn, E. Nemeth, W.I. Sundquist, T. Ganz, G. Musci, J. Kaplan, The molecular mechanism of hepcidin-mediated ferroportin down-regulation, Mol. Biol. Cell. 18 (2007) 2569–2578.
[9] Y.M. Kuo, T. Su, H. Chen, Z. Attieh, B.A. Syed, A.T. McKie, G.J. Anderson, J. Gitschier, C.D. Vulpe, Mislocalisation of hephaestin, a multicopper ferroxidase involved in basolateral intestinal iron transport, in the sex linked anaemia mouse, Gut. 53 (2004) 201–206.
[10] H. Chen, G. Huang, T. Su, H. Gao, Z.K. Attieh, A.T. McKie, G.J. Anderson, C.D. Vulpe, Decreased hephaestin activity in the intestine of copper-deficient mice causes systemic iron deficiency, J. Nutr. 136 (2006) 1236–1241.
[11] H. Chen, Z.K. Attieh, T. Dang, G. Huang, R.M. van der Hee, C. Vulpe, Decreased hephaestin expression and activity leads to decreased iron efflux from differentiated Caco2 cells, J. Cell Biochem. 107 (2009) 803–808.
[12] K.Y. Yeh, M. Yeh, L. Mims, J. Glass, Iron feeding induces ferroportin 1 and hephaestin migration and interaction in rat duodenal epithelium, Am. J. Physiol. Gastrointest. Liver Physiol. 296 (2009) G55–G65.
[13] K.Y. Yeh, M. Yeh, J. Glass, Interactions between ferroportin and hephaestin in rat enterocytes are reduced after iron ingestion, Gastroenterology 141 (2011) 292–299, 299 e291.

[14] H. Chen, T. Su, Z.K. Attieh, T.C. Fox, A.T. McKie, G.J. Anderson, C.D. Vulpe, Systemic regulation of Hephaestin and Ireg1 revealed in studies of genetic and nutritional iron deficiency, Blood 102 (2003) 1893–1899.
[15] K. Kakuta, K. Orino, S. Yamamoto, K. Watanabe, High levels of ferritin and its iron in fetal bovine serum, Comp. Biochem. Physiol. 118 (1997) 165–169.
[16] E.E. Newton, Z. Wu, N.E. Simister, Characterization of basolateral-targeting signals in the neonatal Fc receptor, J. Cell Sci. 118 (2005) 2461–2469.
[17] O. Han, E.Y. Kim, Colocalization of ferroportin-1 with hephaestin on the basolateral membrane of human intestinal absorptive cells, J. Cell Biochem. 101 (2007) 1000–1010.